Carbohydrate Polymers 76 (2009) 188–195

Contents lists available at ScienceDirect

Carbohydrate Polymers

journal homepage: www.elsevier.com/locate/carbpol

Preparation and properties of highly soluble chitosan–L-glutamic acid aerogel derivative

J. Singh [a], P.K. Dutta [a,b,*], J. Dutta [c], A.J. Hunt [b], D.J. Macquarrie [b], J.H. Clark [b]

[a] Department of Chemistry, M.N.National Institute of Technology, Deemed University, Allahabad 211004, India
[b] Green Chemistry Centre of Excellence, Department of Chemistry, University of York, Heslington, York YO10 5DD, UK
[c] Department of Skin and Tissue Engineering, Reliance Life Sciences Centre, Thane Belapur Road, Rabale, Navi Mumbai 400 701, India

ARTICLE INFO

Article history:
Received 7 September 2008
Received in revised form 26 September 2008
Accepted 7 October 2008
Available online 1 November 2008

Keywords:
Water-soluble chitosan
L-Glutamic acid
Conformation
sc.CO_2
FTIR
SEM

ABSTRACT

The objective of this work is to improve the solubility of chitosan at neutral or basic pH using the supercritical carbon dioxide (sc.CO_2). A novel water-soluble chitosan–L-glutamic acid (CL-GA) aerogel derivative was synthesized by reaction of 85% deacetylated chitosan with L-glutamic acid (L-GA) in aq.AcOH subjected to solvent exchange prior to using sc.CO_2 as a nonsolvent for the polymer. The prepared aerogel derivative and molecular conformation of modified chitosan are characterized by using UV, FTIR, ^{1}H NMR, and CD techniques. Some physical properties and surface morphology were analyzed by X-ray diffraction, differential scanning calorimetry (DSC), thermogravimetry (TG), scanning electron microscopy (SEM), transmission electron microscopy (TEM) and porosimetry analysis. Overall, the sc.CO_2 assisted chitosan aerogel derivative opens new perspectives in biomedical applications.

1. Introduction

Chitosan is a partially *N*-deacetylated derivative of chitin, which is commonly found in shells of insects and crustaceans, as well as cell walls of some fungi, and is known as the second most abundant biopolymer in nature after cellulose. Chitosan has been well documented with some advantageous characteristics, including biocompatibility, biodegradability, hydrophilicity, non-toxicity, and nonantigenicity as well as bioadherence and cell affinity (Gong, Zhong, Zhao, & Zhang, 2000; Richardson, Kolbe, & Duncan, 1999). It is being used extensively in pharmaceutical and biomedical areas such as drug delivery vehicles, carriers of immobilized enzymes and cells, biosensors, ocular inserts, artificial organs, orthopedic materials, surgical devices and biodegradable packaging (Bernkop-Schnürch, Humenberger, & Valenta, 1998; Brito & Campana-Filho, 2004; Felse & Panda, 1999; Santos, Dockal, & Cavalheiro, 2005; Varna, Deshpande, & Kennedy, 2004), and in particular, temporary implants for fixations and supports in tissue regeneration, which are commonly known as tissue engineering scaffolds (Khor & Lim, 2003; Rinki, Dutta, & Dutta, 2007; Sasiprapha, Sei-ichi, & Suwabun, 2007).

The cationic nature of chitosan limits the versatility of aqueous solution and pH range because it only dissolves in some specific organic acids including formic, acetic, propionic, lactic, citric and succinic acid, as well as in a very few inorganic acids, such as hydrochloric, phosphoric, and nitric acid (Wang, Turhan, & Gunasekaran, 2004). The solubility of chitosan also depends on the pK_a of these acids and their concentrations. Furthermore, chitosan solution is very viscous even at low concentrations, and its applicability in a commercial context is thus often restricted (Sugimoto, Morimoto, Sashiwa, Saimoto, & Shigemasa, 1998). Hence, improving the solubility of chitosan is crucial if this plentiful resource is to be utilized across a wide pH range. Strategies for improving chitosan solubility can be divided into three methods based on preparation principles. Firstly, homogeneous phase reaction (Sannan, Kurita, & Iwakura, 1976). Secondly, reducing the molecular weight of chitosan produces high solubility. The third and final method of improving solubility involves introducing a hydrophilic functional group to the chitosan, a technique also called the chemical modification method (Holme & Perlin, 1997). Many chitosan derivates including CM-chitosan (carboxymethyl chitosan), *N*-sulfofuryl chitosan, 5-methyl pyrrolidinone chitosan, and dicarboxymethyl and quaternized chitosan – have been developed, with a solubility range of 3–10 g/l obtained (Delben, Muzzarelli, & Terbojevich, 1989; Dung, Milas, Rinaudo, & Desbrieres, 1994; Muzzarelli, 1992; Watanabe, Saiki, Matsumoto, & Azuma, 1992; Heras, Rodriguez, Ramos, & Agullo, 2001; Gomes, Gomes, Batista, Pinto, & Silva, 2008). One of the reasons for the intractability of chitosan lies in the rigid crystalline structure and the acetamido

* Corresponding author.
E-mail address: pkd_437@yahoo.com (P.K. Dutta).

0144-8617/$ - see front matter © 2008 Elsevier Ltd. All rights reserved.
doi:10.1016/j.carbpol.2008.10.011

or primary amino group residues that have an important role in the formation of conformational features through intra and/or intermolecular hydrogen bonding (Nishimura, Kohgo, Kurita, & Kuzuhara, 1991; Dutta & Singh, in press).

sc.CO_2 is a recent technique as a processing solvent in polymer applications such as polymer modification, formation of polymer composites, polymer blending, microcellular foaming, particle production and polymerization (Alsoy & Duda, 1999; Cooper, 2000; Kendall, Canelas, Young, & De Simone, 1999; Romain, Karine, Francoise, & Daniel 2003; Tomasko et al., 2003). Its gas-like diffusivity and liquid-like density in the supercritical phase allow replacing conventional, often noxious solvents with sc.CO_2. It has attracted particular attention as a supercritical fluid in the synthesis as well as processing areas for polymers owing to its attractive physical properties. It is non-toxic, non-flammable, chemically inert and inexpensive. Today the use of sc.CO_2 as a solvent can also be seen in the processing of various biodegradable/biocompatible polymers for pharmaceutical and medical applications in the forms of particles and microcellular foam (Reverchon & Cardea, 2004; Kho, Kalika, & Knutson, 2001; Matsuyama et al., 2001). The low thermal stability of biodegradable polymers and the lack of organic solvents in processing them are the main reasons for the emergence of sc.CO_2 as a replacement solvent.

There are only a few reports concerning chitosan/L-GA derivative available in literature. Poly(L-glutamic acid)-paclitaxel (PG-TXL) is a new water-soluble paclitaxel derivative that has shown remarkable antitumor activity against both ovarian and breast tumors (Chun et al., 1999). The polyL-GA derivatives are also used in chemotherapeutic and anticancer agents using the drug carrier (Yiyu et al., 2001). A chitosan formulation that can be easily administered, is less toxic, and has greater antitumor effect is needed. In this article the modification was done by the formation of amide linkage between NH_2 group of chitosan and COOH group of L-GA and dried using supercritical carbon dioxide (sc.CO_2) to form aerogel. When polypeptides are applied as polyelectrolytes, the polyelectrolyte chitosan derivatives obtained will be very useful in many biomedical applications. Polyelectrolyte chitosan derivatives consisting of chitosan and L-GA may possess advantages of both chitosan and L-GA, and have a broad range of uses in biomedical applications.

2. Experimental

2.1. Materials

The chitosan powder was a product of Sigma–Aldrich and a degree of deacetylation (DD) of 85% and L-glutamic acid (Sigma–Aldrich) were used as such. Carbon dioxide (CO_2) 99.9% purity was sourced from BOC Ltd. and used as such.

2.2. Measurements

The characterization of the chitosan derivative was carried out by using FTIR technique (Bruker ATR), differential scanning calorimetry (DSC) and thermogravimetric analysis (TGA) with STA 600 thermal analyzer. The morphology was studied by using a JEOL JEM-1230 transmission electron microscope (TEM) and a JEOL JSM-5200 scanning electron microscope (SEM) at 80 and 5 kV, respectively. Electronic absorbance spectra (UV) were recorded on UV.1650PC spectrometer using 1.0 cm quartz cell at ambient temperature. CD spectra were recorded on a Jasco J-810 spectropolarimeter in DMSO. The porosity measurement was done by using the Micrometrics Porosimeter: ASAP2010 model. The ^1H NMR spectra for chitosan and CL-GA have been recorded on 500 MHz Jeol FX90Q FTNMR spectrometer using D_2O/DCl and X-ray diffraction (XRD) measurement on powder samples were performed with the Burker AXS General Area Detector Diffraction System (GADDS). Monochromatized Cu Kα radiation ($\lambda = 0.154$ nm) was used. The powder samples were placed in 0.8 diameter Lindemann glass capillaries. The sample-detector distance was 10 cm. The intensity versus scattering-angle (2θ) was plotted.

2.3. Preparation of chitosan derivative

CL-GA hydrogel derivatives were prepared by using chitosan powder (250 mg) dissolve into 1% aqueous acetic acid 37% (w/v). Water-soluble L-GA (50 mg) solution was added slowly to the chitosan gel and stirred for 6 h, until the chitosan solution turned into a more viscous gel and the magnet bar was stopped. The prepared hydrogel was then subjected to solvent-exchange into acetone and ethyl alcohol prior to sc.CO_2 treatment. The solvent-exchange product was placed inside a sealed chamber of the supercritical fluid (SCF) drying reactor (Thorr Co., USA). The temperature and pressure were raised to 40 °C and 100 bar, respectively. Further pressure was raised to 200 bar. The reaction was left for 90 min (Scheme 1) and a flow of CO_2 was then applied through the sample in order to replace all the organic solvent with CO_2. The pressure was then released slowly to the atmosphere. Finally the bluish powdered CL-GA aerogel was obtained.

3. Results and discussion

3.1. FTIR analysis of chitosan, L-GA and CL-GA derivative

Characteristic peaks assignment of chitosan (Fig. 1A) are: 3429 cm^{-1} (O—H stretch overlapped with N—H stretch), 2921 and 2867 cm^{-1} (C—H stretch), 1640 cm^{-1} (amide II band, C—O stretch of acetyl group), 1592 cm^{-1} (amide II band, N—H stretch) 1485–1380 cm^{-1} (asymmetric C—H bending of CH_2 group) and 1035 cm^{-1} (bridge O stretch) of glucosamine residue. The IR spectral band of L-GA (Fig. 1B): 2966 cm^{-1} (O—H stretching), 2855 cm^{-1} for (C—H stretching), 1690 cm^{-1} (C=O group) and 1523 cm^{-1} (N—H stretching of amino group). The (Fig. 1C) shows the significant peak of CL-GA derivative 3110 and 2966 cm^{-1} (axial OH group of chitosan and glutamic acid), 1685 cm^{-1} (amide linkage), 1556 cm^{-1} (N—H bending stretching) and 1067 cm^{-1} (bridge C—O—C stretch) of chitosan residue.

In the IR spectra of chitosan derivative, the strong peak at 1466 cm^{-1} could be assigned to the asymmetry deformation of CH_2, and the C—O adsorption peak of secondary hydroxyl group becomes stronger and move to 1067 cm^{-1} the intensity of primary alcohol 1035 cm^{-1} due to C—O stretching vibration, becomes much smaller than in chitosan. The new peak appears at 2966 indicates the incorporation of the L-glutamic acid moieties. The FTIR results suggest that the COOH group of L-GA have been successfully bonded to the NH_2 group of chitosan main chain to form amide linkage.

The relative FTIR analysis of CL-GA derivative at different pH showed that a strong interaction will not occur at all pH ranges because the relative number of —NH_3^+ groups in chitosan is high and the number of —COO^- groups in L-GA is low at low pH; an opposite trend will appear at high pH. As the number of one ionizing groups increases, the number of the other groups decreases. In CL-GA derivative, lower frequency shifts of amides I and II are found, and as the pH increases, the signal of the —OH group in —COOH of L-GA at 1442 cm^{-1} weakens, and the characteristic absorption band of the C=O group at 1690 cm^{-1} is combined with amide I. This may result from the strong electrostatic interaction between the —COOH of L-GA and the —NH_2 of chitosan. Furthermore, the formation of hydrogen bonds causes the C=O peak to shift to lower

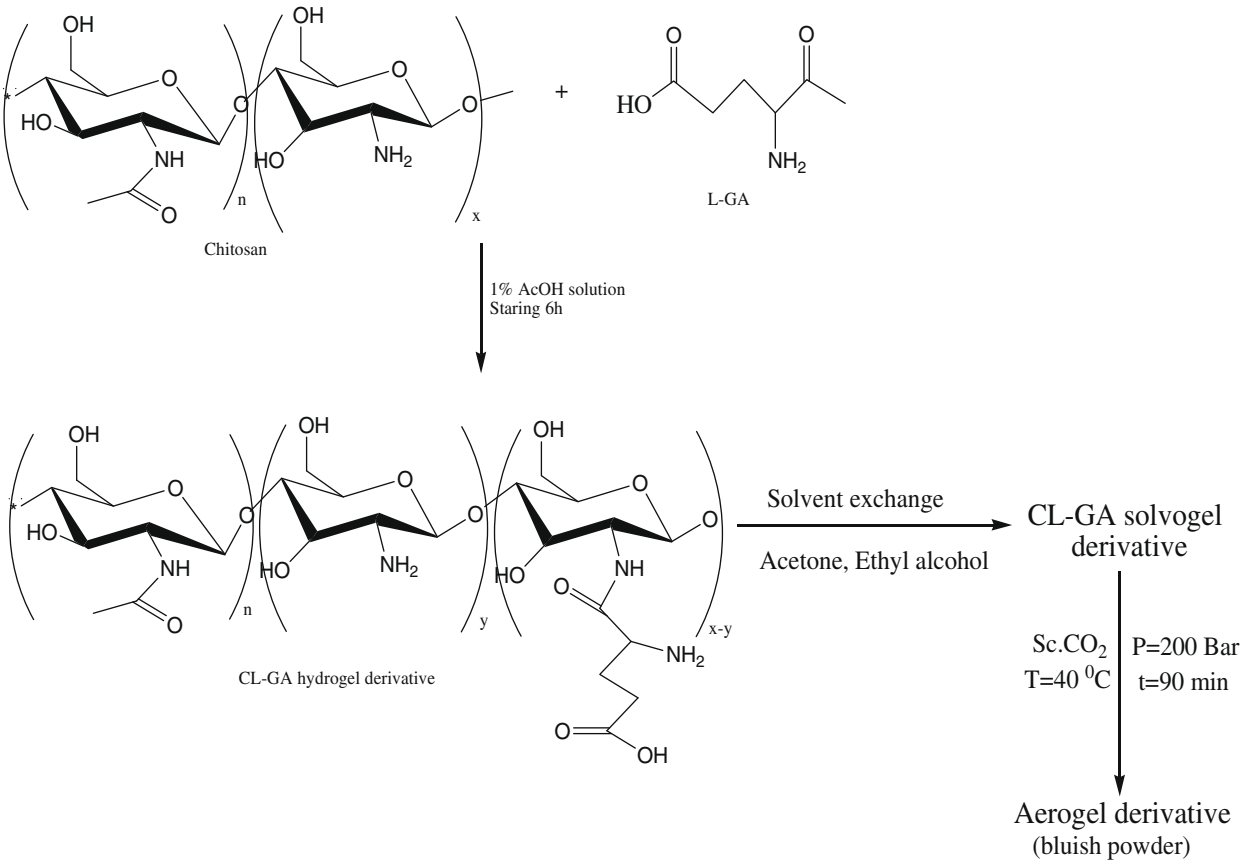

Scheme 1. Preparation of CL-GA acid aerogel derivative by using sc.CO_2.

wavenumber. In most published works, (Berger, Reist, Mayer, Felt, & Gurny, 2004; Schatz, Domard, Viton, Pichot, & Delair, 2004) the peak of the C=O group remained independent in complexes. However, the present result suggests that the peak of the C=O group does not appear independent under all conditions. New peaks appear at 2106 and 1400 cm^{-1} in the spectra of CL-GA derivative at pH 4 and CL-GA derivative at pH 5. These are assigned to the $-NH_3^+$ and $-COO^-$ deformation, respectively, resulting from the blending of the chitosan polymer and L-GA. However, no peaks are found at 2106 cm^{-1} and the absorption at 665 cm^{-1} in CL-GA derivative at pH 3, indicating that the interaction for pH = 3 is very weak. Thus, the results of FTIR analysis clearly prove the formations of the CL-GA derivative are of the acid–base blend.

3.2. ^{1}H NMR analysis

Proton assignment of chitosan (Fig. 2A) is: δ = 4.89 ppm appears for chemical shift of the internal standard, δ = 4.37 ppm is due to chemical shift of the acetal proton (C—H) of the glucosamine overlaps the chemical shift of the internal standard, δ = 3.27 ppm for $-CH-NH_2$ protons (H2), δ = 3.92–3.72 ppm for (H3, H4, H5 and H6) protons of glucosamine ring, δ = 3.27 ppm appear for chemical shifts of (H2) protons and upfield δ = 2.04 ppm for ($-NHCO-CH_3$) acetamido protons. Compared with chitosan, the characteristic proton signals of CL-GA (Fig. 2B) appeared at δ = 3.97–3.55 ppm for (H3, H4, H5 and H6) glucosamine ring, δ = 7.6 ppm for (N—H) protons of amide linkage and a weak signal appear at δ = 5.5 is due to O—H protons.

^{1}H NMR spectra confirm the formation of new amide linkage between NH_2 group of chitosan and COOH group of L-GA under mild condition. A particular case could be used for evaluation of degree of substitution (DS) of chitosan. Protons that belong to L-GA moieties have signals in the region between δ = 3.97 and 3.55 ppm. These signals overlap with the signals of the protons H3—H6 of the chitosan backbone. The DS was about 0.36 per glucose unit, as determined via the calculation of integral ratio of the protons (δ = 3.97–3.22 ppm) of chitosan derivatives and the protons (δ = 2.04 ppm) on the glucosamine unit of chitosan molecules.

3.3. X-ray diffraction study

X-ray diffraction spectra of chitosan and CL-GA derivative show that chitosan (Fig. 3a) exhibits three reflection falls at $2\theta = 11^0$, $2\theta = 20^0$ and $2\theta = 22^0$. Chitosan shows very broad lines especially for the smaller diffraction angles, thereby indicating that long range disorder is found in polymer samples. The broader small angle peaks in chitosan suggests that chitosan derivative exhibits higher long range order. The main diffractive regions in CL-GA (Fig. 3b) are at $2\theta = 21.3^0$, $2\theta = 22^0$ and $2\theta = 25^0$ with the highest peak intensity of about 210, 178 and 137 counts, respectively. Chitosan derivative has higher intensity pattern than chitosan, is due to the presence of lesser DS of L-GA onto chitosan matrix, which indicates that chitosan is substantially more amorphous. X-ray diffraction pattern (XRDP) also displays the line between $2\theta = 11^0$ and 22^0 in chitosan derivative are broader than the narrower lines found at angles $2\theta > 22^0$. This indicates an increase in long-range disorder at small angles. This long range amorphous structure in chitosan gives way to greater short-range order for diffracting atom pairs at $2\theta = 22^0$ (presumably those in the glycosidic rings). This short-range order explains the agreement of the chemical shift tensor shapes between corresponding monomer and polymer samples. XRDP prove here that the crystal lattice has transformed from amorphous structure in to a relatively crystalline structure in chitosan to CL-GA derivative.

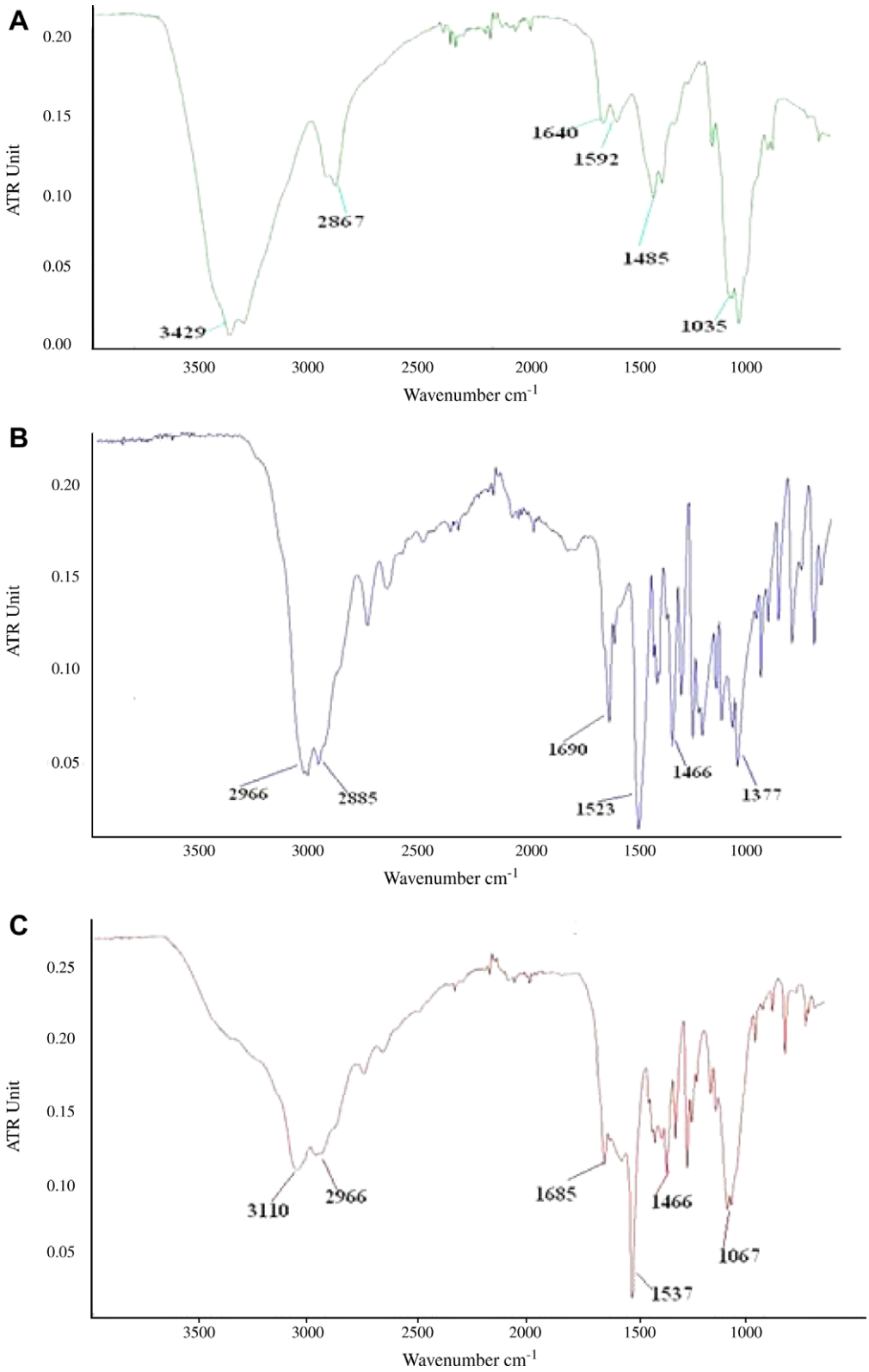

Fig. 1. FTIR spectra of (A) chitosan, (B) L-GA and (C) CL-GA derivative.

3.4. CD and UV spectra of CL-GA derivative

Chitosan itself is transparent in the UV and visible region, and so its conformation is hard to characterize by spectroscopy methods. However, we can overcome this natural handicap by borrowing chromophore from extrinsic molecule. The acid group moieties play the role of reporter molecules for the spectroscopy study, from which the helical conformation is deduced.

Electronic absorbance spectra (UV) of CL-GA derivative (Fig. 4b) show a broad band between the λ = 290–297 nm. The CD spectra of CL-GA derivative (Fig. 4a) in DMSO solution with concentration 50 mg/L exhibit a negative band at λ = 282 nm with −5.74

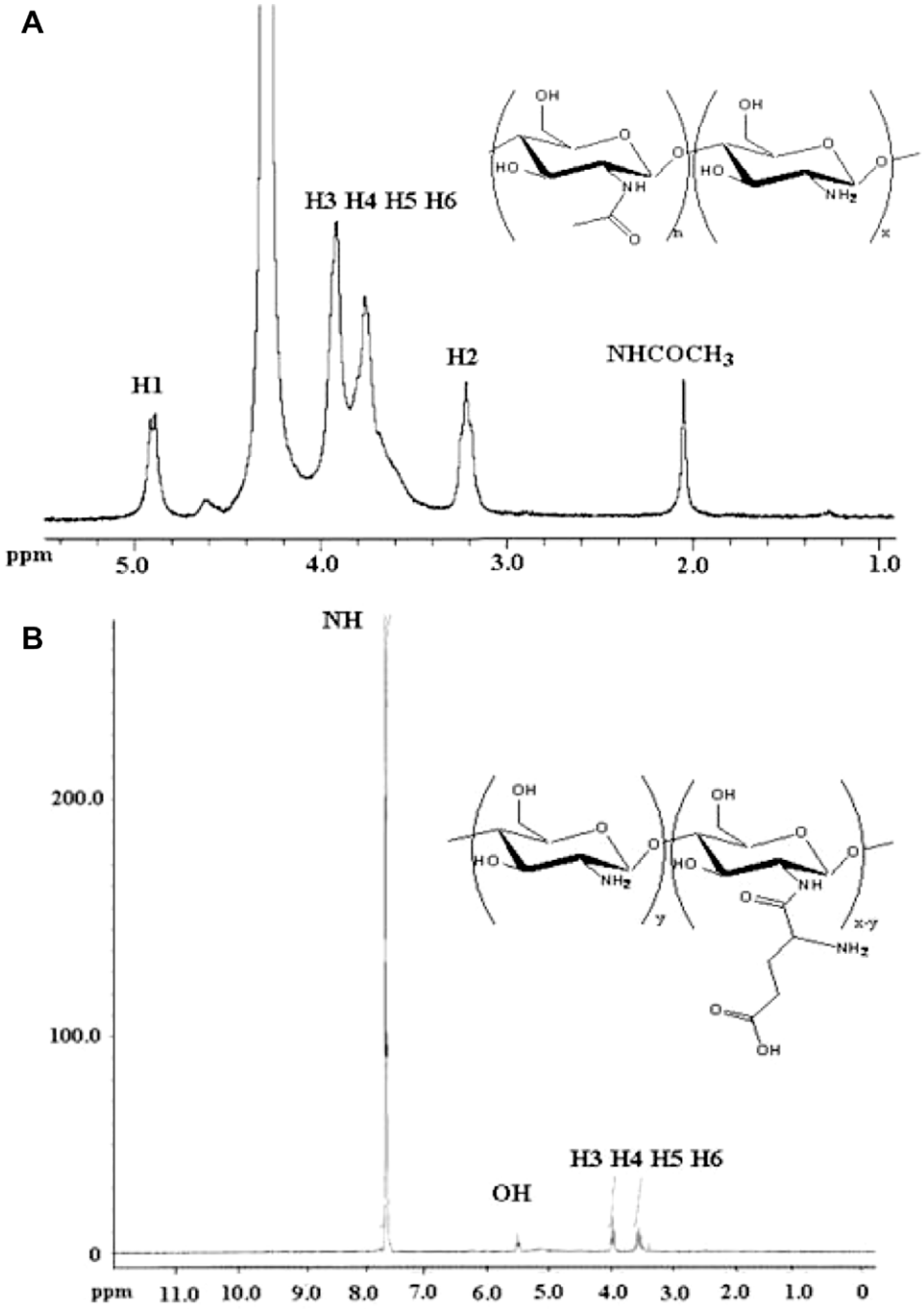

Fig. 2. ^{1}H NMR spectra of (A) chitosan and (B) CL-GA derivative.

ellipticity/mdeg. The negative band is due to electronic dipole transition moment of chromophore (L-GA) as a result of the interaction between the chromophore and the chiral main chain. The CD signals observed in substituted polysaccharide are generally assumed to be induced from chromophore absorbance under the asymmetric interaction of the helical main chain (Harkness & Gray, 1990; Redl, Lutz, & Daub, 2001). The chitosan acid salt derivative is concerned, that observed transition moment are separated from the nearest chiral centre by more than three bonds and are abele to adopt many configuration with respect to the chiral centre because of the rotation of the joining bonds. Here, the rotation about C2 chiral carbon of glucosamine residue, which forms amide linkage with L-GA. In this case, the induced CD will be very weak. Therefore, the contribution of the chiral carbon centre to the chiroptical property of the polymer is negligible. The observed CD signal is simply indicative of the helical conformation of CL-GA derivatives.

3.5. Differential scanning calorimetry and thermo gravimetric analysis

The DSC thermogram of chitosan (Figure not shown) shows a broad endothermic peak around 102.3 °C and sharp exothermic peak at 376.5 °C. The former endothermic peak may be due to the water vapor that the chitosan contains. While the latter may be attributed to the decomposition of chitosan. The sharp endothermic peak of CL-GA (Figure not shown) is 198 °C may be due to the structural arrangement of the lesser DS containing derivative in the main matrix. The broad endothermic peak at

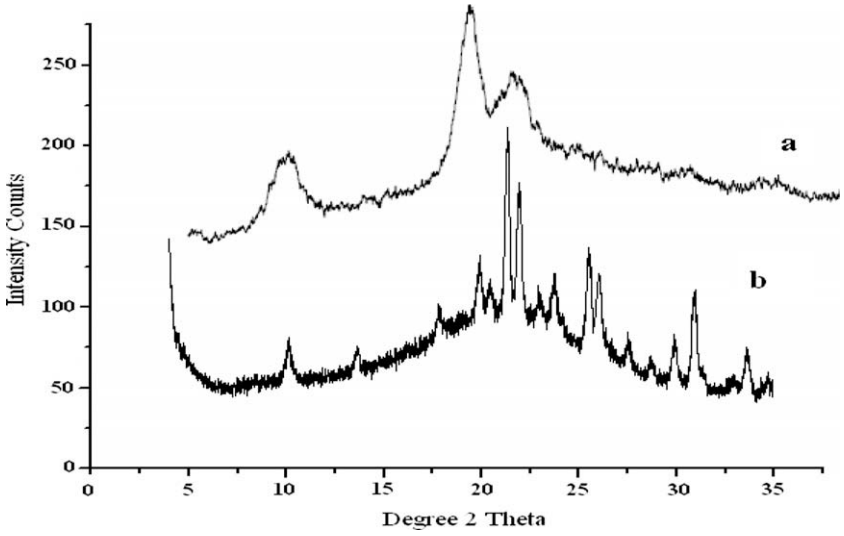

Fig. 3. XRDP of (a) chitosan and (b) CL-GA derivative.

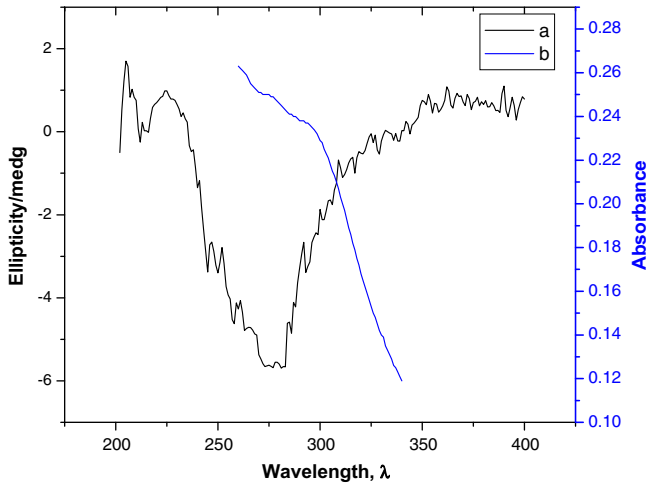

Fig. 4. CD (a) and UV (b) spectra of CL-GA derivative in DMSO solution the polymer concentration was 50 mg/L.

288 °C corresponds to its degree of substitutional changes. The results indicated that the structure of chitosan chains has been changed due to the introduction of glutamic acid and the reduced ability of crystallization. The lack of the exothermic decomposition in CL-GA (present at 376.5 °C in chitosan) provides good evidence towards the successful modification of this material.

The TGA thermograp of chitosan (Figure not shown) shows slow weight loss starting from 140 to 200 °C due to the decomposition of polymer with low molecular weight, followed by more obvious loss of weight starting from 200 to 310 °C, which could be attributed to a complex process including dehydration of the saccharide rings, depolymerization and decomposition of the acetylated and deacetylated units of the polymer (Peniche & SanRoman Arguelles-Monal, 1993). A fast process of weight loss appears in TG curve for CL-GA (Figure not shown) decomposing from 170 to 300 °C, is may be due to the lower grafting of acid in a polymer derivative. The results demonstrate the loss of the thermal stability for CL-GA derivative to the original chitosan. Introduction of glutamic acid group into polysaccharide structure should disrupt the crystalline structure of chitosan, especially through the loss of the hydrogen bonding.

3.6. SEM and TEM analysis

The scanning electron micrographs (SEMs) of the native chitosan are shown in (Fig. 5A and B). It exhibited a nonporous, smooth membranous phases consisting of dome shaped orifices, microfibrils and crystallites. It also exhibited flat lamellar phases on which a large number of protruding microfibrils are evident. The electron micrographs of CL-GA derivative are shown in (Fig. 5C–F). The SEMs of chitosan derivative exhibited a polyphasic microporous structure. L-GA was successfully integrated in to the polymer matrix with no visible agglomerate formation at low particle amounts. SEM images indicated that the struts are formed at the junction of the micro-porous cells and that the struts are oriented randomly in all direction with the strut thickness always much smaller than the cell diameter. The pore dimensions are non-uniform with thin walls and are randomly dispersed in the polymer matrix.

The shape of CL-GA derivative was measured in the solid state using transmission electron microscopy (TEM, Fig. 6). The chitosan derivative formed regularly packed aggregates of spherical particles. The dark lines represent the cross section of the chitosan derivative layer and the gray area corresponds to the matrix. The TEM study is simply an indicative of the helical conformation of chitosan acid derivative.

The morphology of the micro-porous structures formed by phase inversion depends on various thermodynamic and kinetic factors, as well. The phase inversion of semicrystalline polymer derivative is proceeded along with two competitive phenomena: Liquid–Liquid (L–L) and Solid–Liquid (S–L) demixing (Tsivintzelis, Sotirios, Zubur-tikudis, & Panayiotou, 2007). The former leads to uniform microporous structures, while the latter results in spiny or jagged structures that are more interconnected. In all cases presented in SEM Fig. 5, structures with non-uniform cross-sections and micropores were obtained. This indicates L–L demixing as the dominant mechanism. The pores are formed due to the initial nucleation and growth of the polymer-lean phase that occurs inside the polymer-rich phase. The diffusion of the solvent to the polymer-lean phase causes the crystallization of the polymer-rich phase and subsequently the "locking" of the microporous structure.

3.7. Aqueous solubility of CL-GA derivative

A major limitation for practical application of chitosan arises from its insolubility in aqueous media at pH higher than 6 (Koide,

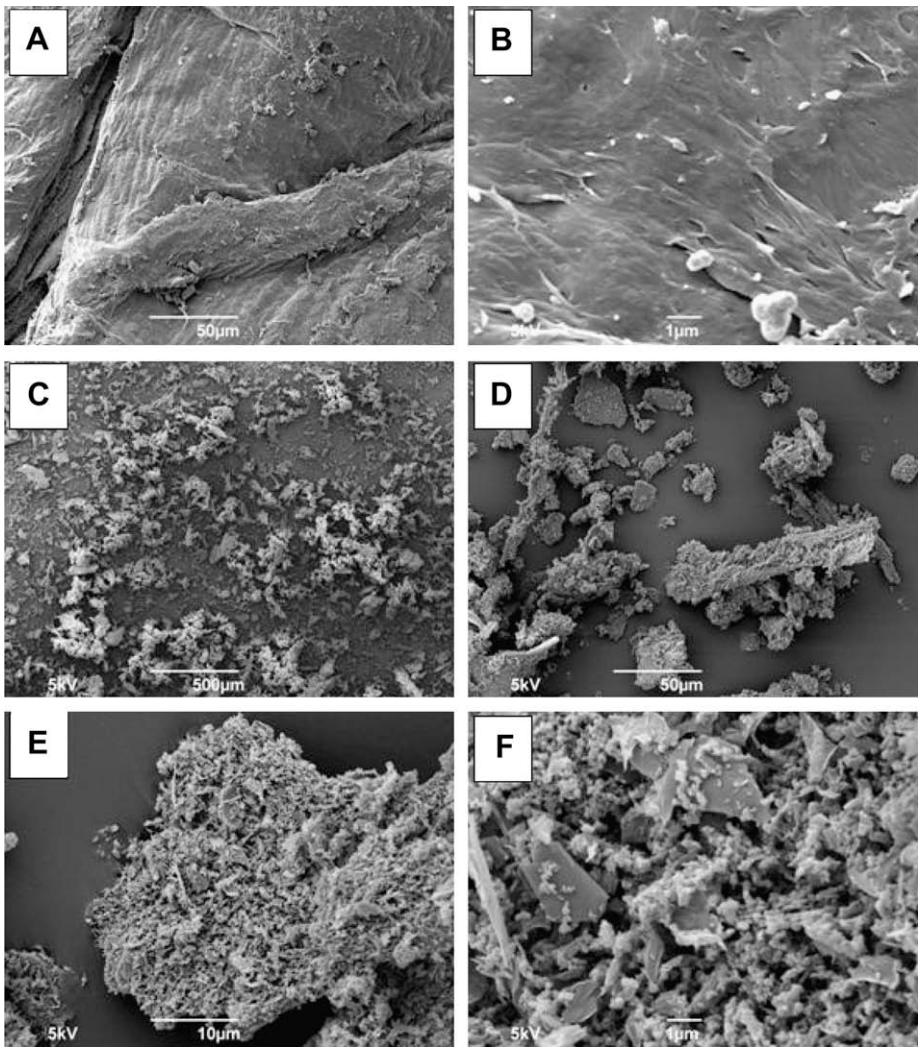

Fig. 5. Scanning electron micrographs of (A) and (B): native chitosan (C–F): CL-GA derivative.

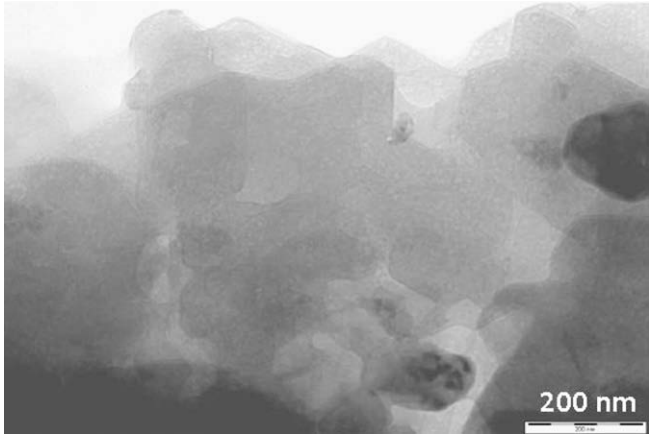

Fig. 6. TEM image of CL-GA derivative.

1998). We had the opportunity to test the solubility of CL-GA derivative in aqueous, acid and alkali solvent at various concentrations and the results are shown in Table 1.

These observation confirm that peptide chitosan derivative herein reported are highly water-soluble up to the concentration of 8% (w/v). On the other hand, it was soluble in the acidic and alkali media at the concentrations of 4% and 5% (w/v), respectively. The solubility was increased due to insertion of more hydrophilic L-GA group at a relatively low DS (~0.36), these novel polymer derivative are obviously soluble at concentration lower than 3% (w/v) and most probably also at concentration higher than 8% (w/v). Thus the development of a water-soluble CL-GA derivative by using sc.CO_2 and examination of its stability characteristic at various concentration is a prerequisite to successful implementation in real-word environment and biomedical applications.

3.8. Porosimetry measurement

By using a Micrometrics Porosimeter (ASAP2010 model) the pore size of the cross section and the average pore diameter of sample were observed. The Brunauer–Emmett–Teller (BET) surface area was calculated using adsorption data in the BET region (P/P_0 = 0.30040457). The pore size distribution of the chitosan derivative was determined from desorption branches of the isotherms by the BJH method. The BJH pore size is defined as the maximum of the BJH pore size distribution (Pandya, Jasra, Newalkar, & Bhatt, 2005). CL-GA demonstrated a BET surface area of 19 m^2/g, with a BJH total pore volume of 0.11 cm^3/g and an average pore diameter (4V/A) of 10.8 nm.

Table 1
Observation of water solubility of different concentrations of CL-GA derivative.

Concentration (%, w/v)	Water	Acetic acid (1%)	NaOH (1%)
3	Soluble	Soluble (immediate)	Soluble (immediate)
4	Soluble (immediate)	Soluble	Soluble
5	Soluble (immediate)	Low viscosity gel	Soluble
6	Soluble (immediate)	Low viscosity gel	Low viscosity gel
7	Soluble (immediate)	Low viscosity gel	Low viscosity gel
8	Soluble (immediate)	Low viscosity gel	Low viscosity gel

4. Conclusions

This study reveals that CL-GA aerogel derivative adopt helical structure in DMSO, as evidence by CD. The conformation of CL-GA derivative depends upon type and size of acid, pH of solution, molecular weight and ionic strength of the solution. The surface morphology, pore structure and diameter of CL-GA aerogel derivative depends on the mutual affinity between sc.CO_2 and organic solvent, but also on process condition. The introduction of L-GA functionalized substituents in the polymeric structure of chitosan yielded novel polymer derivative which is soluble in a wide pH range, which undoubtedly widens the scope of application of chitosan based aerogel in biomedical applications.

Acknowledgments

The authors thank Commonwealth Scholarship Commission-London for providing Academic Staff Fellowship Award-2007 to PKD JS is thankful to Professor Arun B. Samaddar, Director, MNNIT, Allahabad for providing him institute fellowship.

References

Alsoy, S., & Duda, J. L. (1999). Processing of polymers with supercritical fluids. *Chemical Engineering and Technology, 22*, 971–973.

Berger, J., Reist, M., Mayer, J. M., Felt, O., & Gurny, R. (2004). Structure and interactions in chitosan hydrogels formed by complexation or aggregation for biomedical applications. *European Journal of Pharmaceutics and Biopharmaceutics, 57*, 35–52.

Bernkop-Süchnürch, A., Humenberger, C., & Valenta, C. (1998). Basic studies on bioadhesive delivery systems for peptide and protein drugs. *International Journal of Pharmaceutics, 165*, 217–225.

Brito, D., & Campana-Filho, S. P. (2004). A kinetic study on the thermal degradation of *N,N,N*-trimethylchitosan. *Polymer Degradation and Stability, 8*, 353–361.

Chun, L., Janet, E., Price, L. M., Nancy, R., Hunter, S., Dong-Fang, Y., et al. (1999). Antitumor activity of poly (L-glutamic acid)-paclitaxel on syngeneic and xenografted tumors. *Clinical Cancer Research, 5*, 891–897.

Cooper, A. I. (2000). Synthesis and processing of polymers using supercritical carbon dioxide. *Journal of Materials Chemistry, 10*, 207–234.

Delben, F., Muzzarelli, R. A. A., & Terbojevich, M. (1989). Thermodynamic study of the protonation and interaction with metal cations of three chitosan derivatives. *Carbohydrate Polymers, 11*, 205–210.

Dung, P. I., Milas, M., Rinaudo, M., & Desbrieres, J. (1994). Water soluble derivatives obtained by controlled chemical modifications of chitosan. *Carbohydrate Polymers, 24*, 209–215.

Dutta, P. K., & Singh, J. (in press). Conformational study of chitosan: A review. *Proceeding of National Academy of Sciences India, (Section-A), 78*, IV.

Felse, P. A., & Panda, T. (1999). Studies on applications of chitin and its derivatives. *Bioprocess and Biosystems Engineering, 20*, 505–512.

Gomes, P., Gomes, C. A. R., Batista, M. K. S., Pinto, L. F., & Silva, P. A. P. (2008). Synthesis, structural characterization and properties of water-soluble *N*-(γ-propanoyl-amino acid)-chitosans. *Carbohydrate Polymers, 71*, 54–65.

Gong, H., Zhong, Y., Li, J., Gong, Y., Zhao, N., & Zhang, X. (2000). Studied on never affinity of chitosan-derived materials. *Journal of Biomedical Materials Research, 52*, 285–295.

Harkness, B. R., & Gray, D. J. (1990). Preparation and chiroptical properties of tritylated cellulose derivatives. *Macromolecules, 23*, 1452–1457.

Heras, A., Rodriguez, N. M., Ramos, V. M., & Agullo, E. (2001). *N*-Methylene phosphonic chitosan: A novel soluble derivative. *Carbohydrate Polymers, 44*, 1–8.

Holme, K. R., & Perlin, A. S. (1997). Chitosan *N*-sulfate: A water-soluble polyelectrolyte. *Carbohydrate Research, 302*, 7–12.

Kendall, J. L., Canelas, D. A., Young, J. L., & De Simone, J. M. (1999). Polymerizations in supercritical carbon dioxide. *Chemical Review, 99*, 543–564.

Kho, Y. W., Kalika, D. S., & Knutson, B. L. (2001). Precipitation of Nylon 6 membranes using compressed carbon dioxide. *Polymer, 42*, 6119–6127.

Khor, E., & Lim, L. Y. (2003). Implantable applications of chitin and chitosan. *Biomaterials, 24*, 2339–2349.

Koide, S. S. (1998). Chitin-chitosan: Properties, benefits and risks. *Nutrition Research, 18*, 1091–1101.

Matsuyama, H., Yamamoto, A., Yano, H., Maki, T., Teramoto, M., Mishima, K., et al. (2001). Formation of porous flat membrane by phase separation with supercritical CO_2. *Journal of Membrane Science, 194*, 157–163.

Muzzarelli, R. A. A. (1992). Modified chitosan carrying sulfonic acid groups. *Carbohydrate Polymers, 5*, 461–475.

Nishimura, S. I., Kohgo, O., Kurita, K., & Kuzuhara, H. (1991). Chemospecific manipulations of a rigid polysaccharide: Syntheses of novel chitosan derivatives with excellent solubility in common organic solvents by regioselective chemical modifications. *Macromolecules, 24*, 4745–4748.

Pandya, P. H., Jasra, R. V., Newalkar, B. L., & Bhatt, P. N. (2005). Studies on the activity and stability of immobilized α-amylase in ordered mesoporous silicas. *Microporous and Mesoporous Materials, 77*, 67–77.

Peniche, C., & SanRoman Arguelles-Monal, W. (1993). A kinetic study of the thermal degradation of chitosan and a mercaptan derivative of chitosan. *Polymer Degradradation and Stability, 39*, 21–28.

Redl, F. X., Lutz, M., & Daub, J. (2001). Chemistry of porphyrin-appended cellulose strands with a helical structure: Spectroscopy, electrochemistry, and in situ circular dichroism spectroelectrochemistry. *Chemistry European Journal, 7*, 5350–5358.

Reverchon, E., & Cardea, S. (2004). Formation of cellulose acetate membranes using a supercritical fluid assisted process. *Journal of Membrane Science, 204*, 187–195.

Richardson, S. C., Kolbe, H. V., & Duncan, R. (1999). Potential of low molecular mass chitosan as a DNA delivery system: Biocompatibility, body distribution and ability to complex and protect DNA. *International Journal of Pharmaceutical, 178*, 231–243.

Rinki, K., Dutta, J., & Dutta, P. K. (2007). Chitosan based scaffold for tissue engineering. *Asian Chitin Journal, 3*, 69–78.

Romain, V., Karine, M., Francoise, Q., & Daniel, B. (2003). Supercritical CO_2 dried chitosan: An efficient intrinsic heterogeneous catalyst in fine chemistry. *New Journal of Chemistry, 27*, 1690–1692.

Sannan, T., Kurita, K., & Iwakura, Y. (1976). Effect of deacetylation on solubility. *Makromolecular Chemie, 177*, 3589–3593.

Santos, J. E., Dockal, E. R., & Cavalheiro, E. T. G. (2005). Synthesis and characterization of Schiff bases from chitosan and salicylaldehyde derivatives. *Carbohydrate Polymers, 60*, 277–282.

Sasiprapha, P., Sei-ichi, A., & Suwabun, C. (2007). Direct chitosan nanoscaffold formation via chitin whiskers. *Polymer, 48*, 339–400.

Schatz, C., Domard, A., Viton, C., Pichot, C., &. Delair, T. (2004). Versatile and efficient formation of colloids of biopolymer-based polyelectrolyte complexes *Biomacromolecules, 5*, 1882–1892.

Sugimoto, M., Morimoto, M., Sashiwa, H., Saimoto, H., & Shigemasa, Y. (1998). Preparation and characterization of water-soluble chitin and chitosan derivatives. *Carbohydrate Polymers, 36*, 49–59.

Tomasko, D. L., Li, H., Liu, D., Han, X., Wingert, M. J., & Lee, L. J. (2003). A review of CO_2 applications in the processing of polymers. *Industrial and Engineering Chemistry Research, 42*, 6431–6456.

Tsivintzelis, I., Sotirios, I., Zuburtikudis, I., & Panayiotou, C. (2007). Porous poly (L-lactic acid) nanocomposite scaffolds prepared by phase inversion using supercritical CO_2 as antisolvent. *Polymer, 48*, 6311–6318.

Varna, A. J., Deshpande, S. V., & Kennedy, J. K. (2004). Metal complexation by chitosan and its derivates: A review. *Carbohydrate Polymers, 55*, 77–93.

Wang, T., Turhan, M., & Gunasekaran, S. (2004). Selected properties of pH-sensitive, biodegradable chitosan–poly (vinyl alcohol) hydrogel. *Polymer International, 53*, 911–918.

Watanabe, K., Saiki, I., Matsumoto, Y., & Azuma, I. (1992). Abtimetastatic activity of neocarzinostatin incorporated into controlled release gels of CM-chitin. *Carbohydrate Polymers, 17*, 29–33.

Yiyu, Z., Wu, Q., Tansey, W., Chow, D., Hung, M., Charnsangavej, C., et al. (2001). Effectiveness of water soluble poly (L-glutamic acid)–camptothecin conjugate against resistant human lung cancer xenografted in nude mice. *International Journal of Oncology, 18*, 331–336.